WEP Warwick Evans Publishing

International Journal of Mechanical and Electrical Engineering

ISSN: 3005-9615 (Print), ISSN: 3005-7132 (Online) | Volume 5, Number 2, Year 2025
DOI: https://doi.org/10.62051/ijmee.v5n2.05
Journal homepage: https://wepub.org/index.php/IJMEE/index

Optimization of CHB-STATCOM Power Ramp Given Response Time with Capacitance Reduction

Huaen Zhang

School of Electrical Engineering and Automation, Henan Polytechnic University, China
1097148733@qq.com

ABSTRACT

The capacitance-reduced H-bridge cascaded static synchronous compensator (CHB-STATCOM) uses ramp feedforward to suppress the phase-to-phase voltage unbalance of the dc-side voltage when the compensated power jumps, and its minimum transition time T is 10ms, which fails to satisfy the the shortest transition time T is 10ms, which cannot meet the demand of fast response of the device. To address this problem, this paper gives the relationship between the commanded power tapering time T less than 10ms and the inter-phase DC voltage based on the CHB-STATCOM control principle of capacitance reduction. The equations on increasing the DC component under the constraints of the upper and lower boundary constraints are developed and the upper and lower boundary constraints are taken into account under the constraints of the CHB-STATCOM operating principle of decreasing capacitance value .According to the characteristics of the constraint equations, a method for solving the constraint equations is proposed, and the solution results are analyzed by specific examples. The effectiveness of the method in improving the response time is verified by simulation with MATLAB software. The conclusions of the study can also provide a reference for the device to select the power jump time.

KEYWORDS

CHB-STATCOM; Dc-side Voltage Phase-to-phase Unbalance; Power Asymptote; Power Jump Time.

1. INTRODUCTION

As a high-performance reactive power compensation device, the static synchronous compensator has the important role of improving the power factor of the power grid and line transmission capacity. Among them, the Cascaded H-bridge static synchronous compensator (CHB-STATCOM) has the advantages of modularity, easy expansion, and good harmonic characteristics, etc. It has been widely used in power systems[1-4].

The CHB-STATCOM consists of a single-phase structure. As a result, DC capacitors usually require relatively high capacitance values to avoid voltage ripples due to transient power oscillating at twice the industrial frequency[5-6]. This leads to a significant increase in the size of the capacitor. In order to reduce the capacitance and size of capacitors in STATCOM, literature [7-8]suggests to allow relatively large voltage ripples in the capacitor voltage, which can only be realized in compensators that compensate capacitive reactive power.

It is mentioned in the literature [9] that the fluctuating component of the capacitive voltage can be used exclusively for modulation during capacitive operation. The reduction of capacitance tolerance within a certain range does not affect the output capability of the modulation when the peak value of the capacitive voltage is certain. In literature [10], it is mentioned that inductive operation, inductive

Content from this work may be used under the terms of CC BY-NC 4.0 licence (https://creativecommons.org/licenses/by-nc/4.0/).
Published by Warwick Evans Publishing.

operation on capacitor voltage creates an over-modulation problem because of the overlap of the voltage reference on the ac side of the device with the waveform of the capacitor voltage on the dc side and a control scheme is introduced to enhance the operation of the inductive operation in the STATCOM with reduced capacitance.

For reduced capacitance and relatively high voltage ripple, high performance filtering is required to calculate the magnitude of the oscillating capacitor voltage, which is a key factor in capacitor voltage control. In text [10], a band-stop filter is proposed for detecting the peak voltage on the DC side of a STATCOM with reduced capacitance. A more explicit proposal for the use of an analytic filtering scheme can be found in [12-13]. The results show that these methods allow for higher voltage control loop bandwidths compared to conventional low-pass filters.

At the same time, CHB-STATCOM adopts the structure of single-phase cascade of power modules, however, the parallel loss of each power unit, switching loss, and the difference of actual trigger pulse delay to compensate for the sudden power change will cause the three-phase active power inequality and thus lead to the occurrence of phase-to-phase unbalance. In this regard, the existing literature generally adopts zero-sequence voltage or negative-sequence voltage injection method to realize the balance of phase-to-phase DC voltage [14-15], among which the zero-sequence voltage injection method is more widely used in practical engineering because it does not affect the current of the parallel network point [16].

However, for the unbalance caused by the transient behavior of the compensated power, the conventional zero-sequence voltage injection is less effective, and the literature [17] proposes an improved capacitor voltage feed-forward and a suitable reference feedback control to avoid overshooting of the dc-side voltage peaks, but it is not applied to the three-phase system. Literature [18] can effectively suppress this type of phase-to-phase voltage unbalance when using a ramp tapering method and setting the power-given transition time to 10ms.

Literature [18] gives the suppression method, but there are also inappropriate, for example, the use of ramp asymptotic given power method, no matter how much the power jump variable, the transition time is 10ms for some compensation power need to quickly respond to the device is obviously not reasonable.

To address this problem, a method to adjust the transition time according to the before and after leap power and the start leap moment under the upper and lower boundary constraints is given in this paper and verified by simulation and experiment.

2. LOW CAPACITANCE VALUE CHB-STATCOM TOPOLOGY AND CONTROL

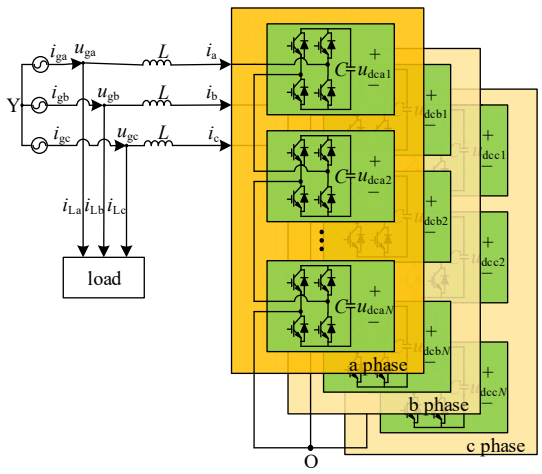


Fig 1. Topology of CHB-STATCOM with reduced capacitance

The topology of the capacitively reduced CHB-STATCOM is shown in Fig. 1, which includes N H-bridge power units per phase.In Fig. 1: u_{dcxj} (j = 1, 2, ..., N, x = a, b, c) is the dc-side voltage of the x-phase power unit j; L is the inductance value of the grid-connected filter; u_{gx} is the three-phase grid voltage; i_{gx} is the three-phase current at the grid side; i_x is the three-phase compensation current of the STATCOM; and i_{Lx} is the three-phase load current.

The control block diagram of CHB-STATCOM with capacitance reduction is shown in Fig. 2, which contains DC side total voltage control, inter-phase DC voltage balance control and intra-phase power unit DC voltage equalization control, reactive power command optimization given, current loop control and carrier phase shift modulation. Among them, reactive power command optimization is the method designed in this paper.

1) CHB-STATCOM DC-side total voltage control with reduced capacitance value

The dc-side voltage diode fluctuation component of the CHB-STATCOM with reduced capacitance value increases and needs to be modulated using the fluctuation voltage, and in order to avoid the large diode fluctuation voltage to increase the device withstand voltage, the peak dc-side voltage needs to be used as the control target. The total DC-side voltage control takes the average value of the squared DC-side voltage of each power unit as the controlled quantity, which is commanded as.

$$U_{\text{const}}^{2*} = u_{\text{dcx_max}}^{2*} - \left| \frac{Q_{\text{ref}}}{3N\omega C} \right| \tag{1}$$

Where: U_{const}^{2*} is the commanded value of the mean DC voltage of the STATCOM power unit, $u_{\text{dcx_max}}^{2*}$ is the commanded value of the squared peak of the DC voltage of the STATCOM power unit. The command value of ω is the fundamental angular frequency, C is the capacitance value of DC side capacitor, Q_{ref} is the command value of STATCOM reactive power. From equation (1), it can be seen that the compensation of reactive power is different, the diode frequency component of the DC side voltage square is different, and the instruction of its control is different.

2) CHB-STATCOM phase-to-phase voltage balancing control with capacitance reduction

In Fig. 2, the discrete sliding Fourier transform is used to extract the DC components of the squared DC-side voltages of phases a and b, which are then differed from the mean value of the squared DC-side voltages of the three phases, and the power increment for phase-to-phase power balancing is obtained through the PI regulator, which in turn is used to find out the zero-sequence voltages required for phase-to-phase voltage balancing.

3) Reactive power command optimization method

In Fig. 2, the reactive power command is optimally given by

$$Q_{\text{ref}} = \begin{cases} Q_{\text{F}} & t < t_0 \\ Q_{\text{F}} - \dfrac{Q_{\text{F}} - Q_{\text{R}}}{T}(t - t_0) & t_0 \le t \le t_0 + T \\ Q_{\text{R}} & t > t_0 + T \end{cases} \tag{2}$$

Where: t_0 is the moment when the STSTCOM power command changes, Q_{F} is the STSTCOM reactive power command before the moment of t_0, Q_{R} is the reactive power command of the device after the moment of t_0, and T is the transition time of the power command ramp fading. The reactive power command is based on the method of ramp wave fading, and in this paper, the transition time T is optimized based on the literature [19].

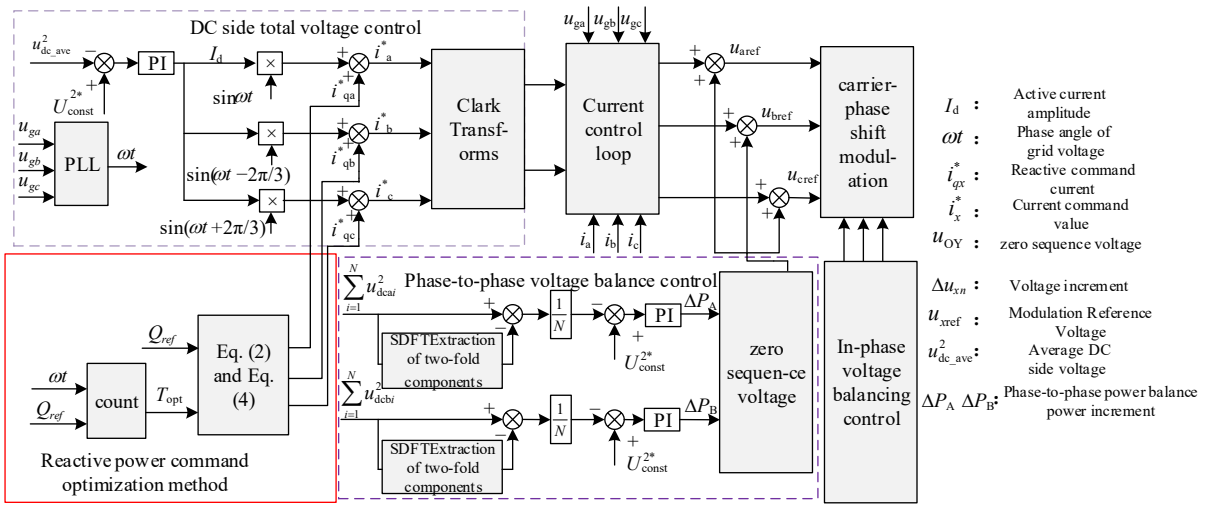


Fig 2. Block diagram of CHB-STATCOM control for capacitance reduction

3. OPTIMIZATION OF THE COMMAND POWER RAMP ASYMPTOTE TIME T

3.1. Formulation of the Command Power Ramp Asymptotic Optimization Problem

From the conservation of power on both sides of the AC and DC sides, it may be assumed that the capacitor voltages in the phases are equal, both $u_{\mathrm{dc}.x}$, it can be seen that the capacitor voltage satisfies

$$NC\frac{\mathrm{d}u_{\mathrm{dc}.x}}{\mathrm{d}t}u_{\mathrm{dc}.x}=u_{x\mathrm{O}}i_x \tag{3}$$

Where: $u_{x\mathrm{o}}$ is the voltage from point x to O in Fig. 1. The fundamental wave component of the output x-phase voltage is approximated by STACOM modulation $u_{x\mathrm{o}}$.

To simplify the analysis and ignore the device losses, let the compensation current be

$$i_x=\frac{2}{3}\frac{Q}{U_{\mathrm{g}}}\sin\left(\omega t+\varphi_x\pm\frac{\pi}{2}\right) \tag{4}$$

Where: U_{g} is the grid voltage amplitude, Q is the STATCOM compensated reactive power, and φ_x is the initial phase angle of the grid voltage.

When Q is positive, the phase of STATCOM compensation current i_x exceeds the phase of PCC point voltage, which is called capacitive condition; when Q is negative, the phase of STATCOM compensation current i_x lags behind the phase of PCC point voltage u_{gx}, which is called inductive condition.

Based on Fig. 1, from the circuit KVL, the fundamental waveform component of the STATCOM modulated output phase voltage can be expressed as

$$u_{x\mathrm{O.ref}}(t)=U_{x\mathrm{O}}\sin\left(\omega t+\varphi_x\right) \tag{5}$$

Where

$$U_{x\mathrm{O}}=U_{\mathrm{g}}+\frac{2\omega LQ}{3U_{\mathrm{g}}} \tag{6}$$

STATCOM compensation reactive power is approximated as the command power, ignoring the control error of the total voltage control on the dc side, the integrated equation (1) ~ equation (6) can

be obtained as the expression of the dc-side voltage when the power is given by using the ramp gradient method as follows

$$u_{\mathrm{dcx}}^2(t)\begin{cases}-\dfrac{Q_{\mathrm{F}}}{3\omega NC}\cos(2\omega t+2\varphi_x)+u_{\mathrm{constF}}^2 & ,t<t_0\\ -\dfrac{Q_{\mathrm{F}}}{3\omega NC}\cos(2\omega t+2\varphi_x)+\dfrac{Q_{\mathrm{R}}-Q_{\mathrm{F}}}{6\omega^2 NCT}\left[\sin(2\omega t+2\varphi_x)-\sin(2\omega t_0+2\varphi_x)\right]-\dfrac{Q_{\mathrm{R}}-Q_{\mathrm{F}}}{3\omega NCT}(t\text{-}t_0)\cos(2\omega t+2\varphi_x)\\ +u_{\mathrm{constF}}^2-\dfrac{u_{\mathrm{constF}}^2-u_{\mathrm{constR}}^2}{T}(t-t_0) & ,t_0\le t\le t_0+T\\ -\dfrac{Q_{\mathrm{R}}}{3\omega NC}(\cos(2\omega t+2\varphi_x)+u_{\mathrm{constR}}^2+\dfrac{Q_{\mathrm{R}}-Q_{\mathrm{F}}}{6\omega^2 NCT}[\sin(2\omega(t_0+T)+2\varphi_x)-\sin(2\omega t_0+2\varphi_x)] & ,t>t_0+T\end{cases} \tag{7}$$

Where:

$$\begin{cases}u_{\mathrm{constF}}^2=u_{\mathrm{dcx_max}}^{2*}-\left|\dfrac{Q_{\mathrm{F}}}{3N\omega\mathrm{C}}\right|\\ u_{\mathrm{constR}}^2=u_{\mathrm{dcx_max}}^{2*}-\left|\dfrac{Q_{\mathrm{R}}}{3N\omega\mathrm{C}}\right|\end{cases} \tag{8}$$

From Eq. (7), the increase in the amount of direct current in the squared value of the voltage on the DC side of each phase after the end of the transition process is

$$\Delta u_{\mathrm{dcx_1}}^2=\frac{Q_{\mathrm{R}}-Q_{\mathrm{F}}}{3\omega NC}\frac{[\sin(2\omega(t_0+T)+2\varphi_x)-\sin(2\omega t_0+2\varphi_x)]}{2\omega T} \tag{9}$$

Literature [19] demonstrated that when T is 10ms, the increased direct current in the squared value of the three-phase DC side voltage is zero, however, this reduces the dynamic response time of the STATCOM power, which is a key performance indicator of the device. From the engineering practice, the device design allows a certain overshoot of the DC side voltage, and the DC side voltage withstand has a certain margin. In this paper, the allowable overshoot of the DC-side voltage is used as a constraint to optimize the transition time T of the power command ramp asymptote in order to improve the response time of STATCOM reactive power compensation.

The transition time T of the power command ramp asymptote should be selected so that the peak DC-side voltage during the compensation power change satisfies the design constraints. Defining the CHB-STATCOM dc-side voltage peak multiplier as k, the dc-side voltage peak during the power change is required to satisfy

$$u_{\mathrm{dcx_P}}\le ku_{\mathrm{dcx_max}}^* \tag{10}$$

At the same time, the modulation is effective during the transition process, and the DC side voltage needs to satisfy the

$$u_{\mathrm{dcx}}(t)\ge\left|\frac{u_{x\mathrm{O.ref}}(t)}{N}\right| \tag{11}$$

To enhance the reactive power response time of the device, the transition time T should be such that the dc-side voltage satisfies the constraints of Eqs. (10) and (11) and the time T should be minimized.

3.2. Establishment of the Command Power Ramp Asymptotic Optimization Objective

From Eq. (6), the dc-side voltage is divided into three stages when the commanded power ramp asymptote is used. Defined $t<t_0$ as before transition, $t_0\le t\le t_0+T$ as during transition and $t>t_0+T$ as after transition. The DC side voltage in the transition and the post-transition phase satisfies the constraints of Eqs. (10) and (11), and the optimization objective of the command power ramp

transition time T under the constraints of Eqs. (10) and (11) is proposed to be established for the two phases in this section, respectively.

1) Optimization Target Establishment for Temporal Transition Time T at $t > t_0 + T$

From equation (7), the square of the peak DC side voltage can be expressed

$$u_{\mathrm{dcx_P}}^2 = \Delta u_{\mathrm{dcx_1}}^2(T) + u_{\mathrm{dcx_max}}^{2*} \qquad t > t_0 + T \tag{12}$$

The dc-side voltage satisfies the constraint of Eq. (8) equals to

$$u_{\mathrm{dcx_P}}^2 \le \left(k u_{\mathrm{dcx_max}}^*\right)^2 \tag{13}$$

Combining Eqs. (12) and (13) yields

$$\Delta u_{\mathrm{dcx_1}}^2(T) \le (k^2 - 1) u_{\mathrm{dcx_max}}^{2*} \tag{14}$$

That is, the DC side voltage satisfies the constraint of Eq. (10) after the transition, and the optimization objective of the transition time T is Eq. (14).

The dc-side voltage satisfies the constraint of equation (11) is equivalent to

$$u_{\mathrm{dcx}}^2(t) \ge \frac{u_{x\mathrm{O.ref}}^2(t)}{N^2} \qquad t > t_0 + T \tag{15}$$

Let Eq. (15) read

$$f(t) = N^2 u_{\mathrm{dcx_1}}^2(t) - u_{x\mathrm{O.ref}}^2(t) \ge 0 \tag{16}$$

Substituting Eq. (5) and Eq. (7) into Eq. (16) yields

$$\begin{aligned} &\left(\frac{U_{x\mathrm{O}}}{2N^2}^2 - \frac{Q_{\mathrm{R}}}{3N\omega C}\right)\cos(2\omega t + 2\varphi_x) \\ &-\frac{U_{x\mathrm{O}}}{2N^2}^2 + \Delta u_{\mathrm{dcx_1}}^2(T) + u_{\mathrm{dcx_max}}^{*2} - \left|\frac{Q_{\mathrm{R}}}{3N\omega \mathrm{C}}\right| \ge 0 \end{aligned} \tag{17}$$

Let the coefficient of the term $\cos(2\omega t + 2\varphi_x)$ in Eq. (17) be

$$w = \frac{U_{x\mathrm{O}}}{2N^2}^2 - \frac{Q_{\mathrm{R}}}{3N\omega C} \tag{18}$$

Literature [18] mentions that w should not be less than zero due to the constraints on the tolerance value taken by the STATCOM with reduced tolerance.

(1) Tolerant operating conditions after transition

Satisfying (16) is equivalent to the minimum value of the function $f(t)$ is greater than or equal to zero. From equation (17): the function $f(t)$ minimizes when

$$f(t)_{\min} = -\frac{U_{x\mathrm{O}}^2}{N^2} + \Delta u_{\mathrm{dcx_1}}^2(T) + u_{\mathrm{dcx_max}}^{2*} \ge 0 \tag{19}$$

From equation (19), we have

$$\Delta u_{\mathrm{dcx_1}}^2(T) + u_{\mathrm{dcx_max}}^{2*} \ge \frac{U_{x\mathrm{O}}^2}{N^2} \tag{20}$$

The left side of the inequality is the peak value of the post-transition DC side voltage, and the right side is the square of the peak value of the output fundamental voltage of each power unit. Therefore, the peak value of the post-transition dc-side voltage will be greater than or equal to the peak value of

the fundamental wave component of the STATCOM modulated output phase voltage in the capacitive condition, which can satisfy equation (15).

That is, the DC side voltage satisfies the constraint of Eq. (11) after the transition, and the optimization objective of the transition time T during capacitive operation is Eq. (20).

(2) Sensible working conditions after the transition

w is constantly greater than zero, the function $f(t)$ can be minimized as

$$f(t)_{\min} = -\frac{U_{xO}^2}{N^2} + \Delta u_{\mathrm{dcx_1}}^2 + u_{\mathrm{dcx_max}}^{2*} - \left|\frac{2Q_{\mathrm{R}}}{3N\omega \mathrm{C}}\right| \geq 0 \tag{21}$$

From Eq. (21)

$$\Delta u_{\mathrm{dcx_1}}^2 + u_{\mathrm{dcx_max}}^{2*} + \frac{2Q_{\mathrm{R}}}{3N\omega \mathrm{C}} \geq \frac{U_{x\mathrm{O}}^2}{N^2} \tag{22}$$

The left side of Eq. (22) is the valley value of the post-transition DC side voltage, and the right side is the square of the peak value of the output fundamental voltage of each power unit. Therefore, the inductive condition will be the post-transition dc-side voltage valley value is greater than or equal to the peak value of the fundamental wave component of the STATCOM modulated output phase voltage, which can satisfy equation (15).

That is, the DC side voltage satisfies the constraint of Eq. (11) after the transition, and the optimization objective of the transition time T during inductive operation is Eq. (22).

2) Optimization constraints established for transition time T at time $t_0 \leq t \leq t_0 + T$

From Eq. (7), when the power before and after the jump and the beginning of the transition time is known, the DC voltage in the transition is only related to the transition time *T*. When the transition time T is selected with the post-transition as the optimization constraint, the resulting T needs to make the DC voltage in the transition also satisfy the constraints of Eq. (10).

$$(ku_{\mathrm{dcx_max}}^*)^2 \geq u_{\mathrm{dcx}}^2(t) \quad t_0 \leq t \leq t_0 + T \tag{23}$$

and Eq. (11) constraints

$$u_{\mathrm{dcx}}^2(t) \geq \frac{u_{x\mathrm{O.ref}}^2(t)}{N^2} \qquad t_0 \leq t \leq t_0 + T \tag{24}$$

Let Eq. (23) read

$$f_1(t) = (ku_{\mathrm{dcx_max}}^*)^2 - u_{\mathrm{dcx}}^2(t) \geq 0 \tag{25}$$

Similarly let Eq. (24) read

$$f_2(t) = u_{\mathrm{dcx}}^2(t) - \frac{u_{x\mathrm{O.ref}}^2(t)}{N^2} \geq 0 \tag{26}$$

Derivation of Eqs. (25) and (26) with respect to t yields the possible extreme points t_1 and t_2 respectively . The solution procedure is shown in the Appendix, substituting the possible extreme points into Eqs. (24)(25), if it satisfies

$$f_1(t_1) = (ku_{\mathrm{dcx_max}}^*)^2 - u_{\mathrm{dcx}}^2(t_1) \geq 0 \tag{27}$$

$$f_2(t_2) = u_{\mathrm{dcx}}^2(t_2) - \frac{u_{x\mathrm{O.ref}}^2(t_2)}{N^2} \geq 0 \tag{28}$$

then it shows that the selected shortest transition time T is valid. That is, the DC-side voltage satisfies the constraints of Eqs. (10) and (11) in the transition, and the optimization objectives of the transition time T are Eqs. (27) and (28), respectively.

3.3. Solution for Minimizing the Transition Time T under Constraints

The solution to minimize the transition time T based on the constraints of Sections 2.1 and 2.2 is shown in Fig. 3.

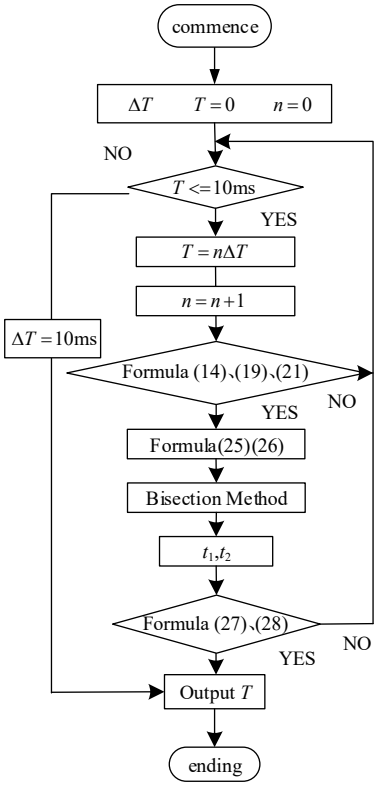


Fig 3. Flowchart for solving

In the figure: ΔT is the step length of each iteration, the step length of the iteration is set according to the need for accuracy, the size of the step length affects the accuracy and computation time, the larger the step length, the smaller the accuracy, the longer the computation time required. Substituting the values obtained from each iteration into Eqs. (14), (19) and (21), the values obtained satisfy the inequality, which indicates that the constraints are satisfied after the transition. Substitute the output into Eqs. (25) and (26), and then substitute the possible extreme points t_1 and t_2 in the transition obtained by dichotomy into Eqs. (27) and (28) to verify whether the DC voltage in the transition satisfies the constraints, and if it does, it is the optimal transition time. If it has not been satisfied then T=10ms is taken for transition.

4. CALCULATED EXAMPLE ANALYSIS AND SIMULATION VERIFICATION

4.1. Example Analysis

Based on the above discussion basic parameters are selected from Table 1.

Table 1. Parameters of the algorithm

parameters	value
RMS grid line voltage U_s/kV	6
compensation capacity Q/Mvar	3
STATCOM rated compensation current peak i_x/A	408
Filter reactance value L/mH	4.5
Module DC Side Capacitance Tolerance C/μF	1600
Pre-transition reactive power compensation Q_F/Mvar	-1
Post-transition reactive power compensation Q_R/Mvar	-2-3
DC side voltage peak control value u_{dc_max}/V	1022
The value of k in Eq. (18)	1.18

After substituting the optimization method proposed in Chapter 2 to solve the problem, it can be obtained that when the pre-transition compensation power Q_F is determined, the three-dimensional relationships of the power post-transition compensation power Q_R, the power leaping moment, the shortest transition time T, and the relationship between the power leaping variable and the shortest transition time T are shown in Figs. 4 and 5, respectively.

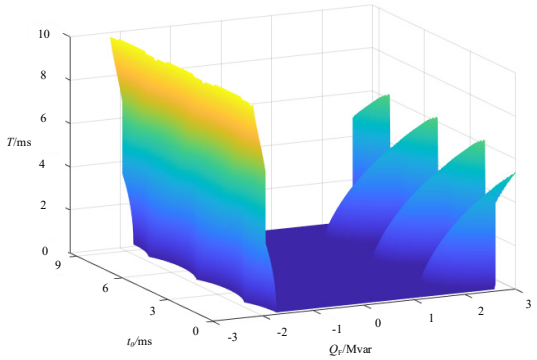


Fig 4. Relationship between power jump moment t_0, Q_A shortest transition time T

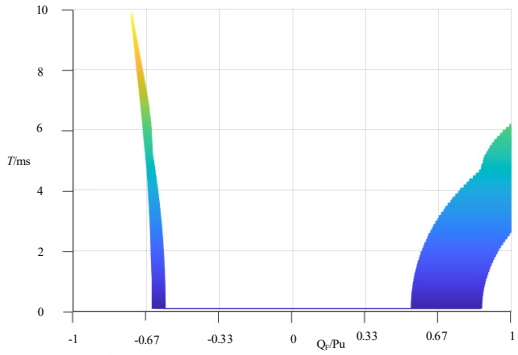
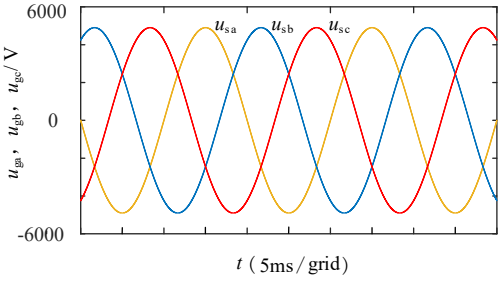


Fig 5. Q_A versus the shortest transition time T

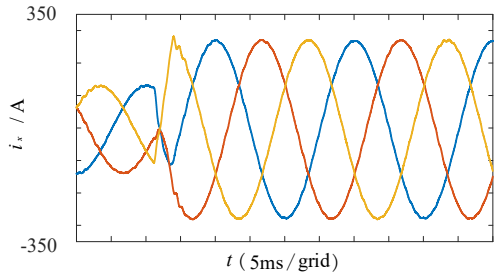
From the analysis of the simulation results in Fig. 5, it can be seen that the optimal transition time of the system shows a positive correlation with the post-transition power, i.e., the optimal transition time is gradually extended with the increase of the post-transition power. At the same time, the selection

of the power leap moment has an effect on the transition time T, which is different at different leap moments t_0.

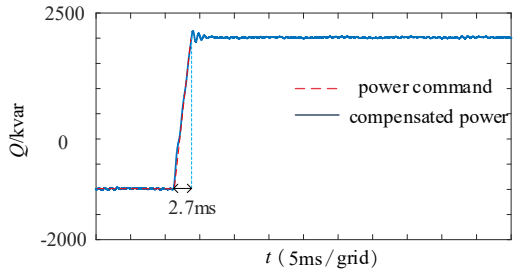
4.2. Simulation Analysis



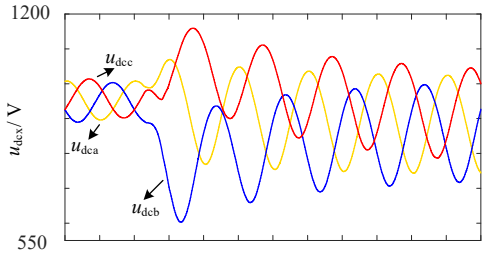
(a) Three-phase grid voltage



(b) Three-phase compensation current



(c) STATCOM power command and compensation power



(d) Three-phase DC side voltage

Fig 6. Simulation results of power change inductive to capacitive

In order to verify the effectiveness of the theoretical analysis and the proposed transition time optimization method in this paper, Matlab/Simulink was used to build a CHB-STATCOM simulation model with reduced capacitance, and the simulation parameters were adopted from the parameters in Table 1, and the control method in Fig. 2 was adopted, with the carrier frequency set to 2000 Hz.

The correctness of the constraint equations established when the transition is capacitive condition, Fig. 6 Simulated waveforms of the pre-set power leapfrog from inductive 1Mvar to capacitive 2Mvar.

The power command starts to change at ωt_0=198°, and the theoretical tapering time T is calculated to be 2.7ms by the method of Chapter 2.Fig. 6(a) shows the three-phase grid voltage, and Fig. 6(b) shows the three-phase compensation current of the CHB-STATCOM. Fig. 6(c) shows the power command and actual compensated power of CHB-STATCOM. From Fig. 6(b) and Fig. 6(c), it can be seen that there is no overshooting of the current during the dynamic process and the power tracking command is very effective. Fig. 8(d) shows the three-phase dc-side voltage, and from Fig. 6(d), it can be seen that the peaks and valleys of the three-phase dc-side voltage are within the constraints of Eq. (10) and Eq. (11). The above simulation proves the effectiveness of the ramp-given response time optimization established in this paper, which achieves the balance between power response time and suppressing the phase imbalance on the DC side.

5. CONCLUSION

In this paper, the CHB-STATCOM with reduced capacitance value is taken as the research object to analyze the influence of the ramp asymptotic power change on the phase-to-phase voltage balance, and the constraint equations are established based on the increased DC component after the transition, and the constraint equations under the constructed constraints are used to carry out the simulation analysis and experimental study, which verifies that the constraint equations are established correctly, and that the response time of power feeding is optimized, and that it does not affect the unit's Effective operation of the device is not affected.

REFERENCES

[1] A. Darvishzadeh, H. Iman-Eini and Y. Neyshabouri, "Diagnosis and Ride Through of Single-Switch Open-Circuit Fault in Low-Capacitance STATCOM," in IEEE Transactions on Power Electronics, vol. 40, no. 1, pp. 1952-1963.

[2] H. Wang, R. Qiu, J. Wu, M. Ma, F. Li and X. Zhang, "Online Capacitor Condition Monitoring for Cascaded-H-Bridge Type Converters," in IEEE Transactions on Power Electronics, vol. 39, no. 10, pp. 12514-12522.

[3] Y. Neyshabouri and H. Iman-Eini, "A New Fault-Tolerant Strategy for a Cascaded H-Bridge Based STATCOM," in IEEE Transactions on Industrial Electronics, vol. 65, no. 8, pp. 6436-6445.

[4] Rodriguez E,et al.Enhancing Inductive Operation of Low-Capacitance Cascaded H-Bridge StatComs Using Optimal Third-Harmonic Circulating Current[J].IEEE Transactions on Power Electronics,2021,36(9):10788-10800.

[5] Wang H,Blaabjerg F.Reliability of capacitors for DC-Link applications in power electronic converters-an overview[J].IEEE Transactions on Industry Applications,2014,50(5):3569-3578.

[6] Liu Q,Rodriguez E,Farivar G ,et al.Discontinuous Modulation of a Cascaded H-Bridge Low-Capacitance StatCom[J].IEEE Transactions on Power Electronics,2022,37(3):2790-2800.

[7] Isobe T,Zhang L,Tadano H,et al.Control of DC-capacitor peak voltage in reduced capacitance single-phase STATCOM [C].2016 IEEE 17th Workshop on Control and Modeling for Power Electronics (COMPEL), Trondheim, Norway, 2016:1-8.

[8] G. Farivar et al., “Load adaptive cascaded H-bridge low capacitance statcom with modular capacitors,” in Proc. 45th Ann. Conf. IEEE Ind. Electron. Soc., Lisbon, Portugal, 2019, pp. 3541–3546.

[9] Isobe T, Shiojima D, Kato K, et al. Full-Bridge reactive power compensator with minimized equipped capacitor and its application to static var compensator[J]. IEEE Transactions on Power Electronics, 2015, 31(1): 224-234.

[10] X. Ge and F. Gao, "Flexible Third Harmonic Voltage Control of Low Capacitance Cascaded H-Bridge STATCOM," in IEEE Transactions on Power Electronics, vol. 33, no. 3, pp. 1884-1889.

[11] Isobe T,Zhang L,Tadano H,et al.Control of DC-capacitor peak voltage in reduced capacitance single-phase STATCOM [C].2016 IEEE 17th Workshop on Control and Modeling for Power Electronics (COMPEL), Trondheim, Norway,2016:1-8.

[12] Farivar G,Hredzak B,Agelidis V G.Reduced-Capacitance Thin-Film H-Bridge Multilevel STATCOM Control Utilizing an Analytic Filtering Scheme[J].IEEE Transactions on Industrial Electronics,2015,62(10):6457-6468.

[13] Rodriguez E,Leyva R,Townsend D,et al.Closed-Loop Analytic Filtering Scheme of Capacitor Voltage Ripple in Multilevel Cascaded H-Bridge Converters[J].IEEE Transactions on Power Electronics,2020,35(8):8819-8832

[14] CHEN H C, CHENG PT. A DC bus voltage balancing technique for the cascaded H-bridge STATCOM with improved reliability under grid faults [J]. IEEE Transactions on Industry Applica-tions, 2017,53(2):1263.

[15] D. Lu, S. Wang, J. Yao, T. Yang and H. Hu, "Cluster Voltage Regulation Strategy to Eliminate Negative-Sequence Currents Under Unbalanced Grid for Star-Connected Cascaded H-Bridge STATCOM," in IEEE Transactions on Power Electronics, vol. 34, no. 3, pp. 2193-2205.

[16] MAHAR JAN L,YAMAGISHI T,AKAGIH. Active-power control of individual converter cells for a battery energy storage system based on a multilevel cascade PWM converter[J].IEEE Transactions on Power Electronics, 2012, 27 (3): 1099.

[17] M. Akihiro, T. Mannen and T. Isobe, "Dynamic Performance Improvement of Model-Based Capacitor Voltage Control for Single-Phase STATCOM with Reduced Capacitance," 2021 IEEE Applied Power Electronics Conference and Exposition (APEC), Phoenix, AZ, USA, 2021, 2024-2029.

[18] DU Shaotong, LI Wei, ZHOU Juan, et al. Analysis and Suppression Mechanism for Clustered Voltage Imbalance Generated by Capacitance Reduction of CHB-STATCOM [J]. Power System Technology,2024,48(11):4628-4637.

[19] DU Shaotong, TAN Xingguo, ZHOU Juan. Capacitor Value Selection Analysis and DC Voltage Control for Cascaded H-Bridge STATCOM With Reduced Capacitance Value [J]. Power System Technology, 2019, 43(1):275-284.